

Quantitative Evaluation of Rotating Short-Axis (RSA) EPI for High Spatial Resolution Diffusion MRI

Yu-Chien Wu¹

¹Radiology and Imaging Sciences, Indiana University School of Medicine, Indianapolis, IN, United States

Target audience: MRI physicists, scientists interested in diffusion MRI, neuroscientists, and brain imaging researchers.

Purpose

Diffusion MRI (dMRI) probes the microstructures of the human brain by measuring diffusion functions of water molecules. dMRI experiments are performed using various approaches depending on the number of both diffusion-weighting (DW) directions and b-value shells. Clinical applications for advanced dMRI experiments are limited due to the scan time and considerable requirements of high-quality imaging: the signal-to-noise ratio (SNR) is crucial for non-linear and complicated computations of diffusion models; high spatial resolution decreases partial voluming artifacts from mixed tissue types; and minimal image distortion provides better anatomy and registration results. Unfortunately, despite their fast imaging speed, conventional single-shot spin-echo EPI (SS-SE-EPI) sequences have long echo times and geometric distortions that prevent high spatial resolution and high-quality dMRI. A new sequence, Rotating Short-Axis (RSA) EPI¹, may address some of the issues associated with SS-SE-EPI and facilitate studies with advanced dMRI. RSA EPI is faster than SS-SE-EPI with a higher SNR and minimal geometric distortion at 1.5^3 and 1 mm^3 voxel resolution¹. Here, computer simulations were performed to quantitatively evaluate RSA methods with respect to effective image resolution, artifacts, and directional estimates of white matter (WM) fiber orientations.

Methods

RSA: In RSA, only one short-axis EPI “blade” covering the central part of the k-space is acquired per DW direction and the blade rotates along with switching the DW directions¹. Echo time thus decreases, resulting in a high SNR and a faster scan time due to partial k-space sampling than in SS-SE-EPI. The short-axis blades decrease EPI geometric distortion². High nominal resolution is achieved along the phase encoding direction and an effective isotropic resolution is achieved through composite reconstruction. **Composite Reconstruction:** For each DW direction, the k-space blades are aligned, centered, and phase-corrected prior to constructing the collective high-resolution composite image. The high-resolution composite image “trains” the individual low-resolution blade images (Fig. 1a), leading to high-resolution RSA images (Fig. 1b). **Simulation:** Shepp-Logan brain phantoms with various isotropic diffusions (Fig. 2) were used to study the image artifacts arising from the blade sampling and composite reconstruction. RSA acceleration factors (AF) of 2, 4, 8, 16, and 32 were simulated at different isotropic voxel sizes (1 , 1.5^3 , and 2^3 mm^3) and different SNR levels (infinity, 30, 20, 15, 10, and 5). A quadratic Gaussian noise was added to create Rician noise in the magnitude images. Images of full k-space sampling mimicking SS-SE-EPI acquisition were also simulated for comparison. To study the effective resolution from the blade sampling and composite reconstruction, we simulated a digital phantom of a delta function as an ideal point-spread function (PSF). Effective resolution is defined as the full width at half-maximum (FWHM) of the reconstructed PSF in the image space. Directional estimates of WM fiber orientation were evaluated by a post-processing computer simulation on human brain data. HARDI with 492 DW directions and 3000 s/mm^2 b-value was performed on a healthy human volunteer with a 3.0T Philips Achieva scanner. The full k-space SS-SE-EPI sequence was used as a “pseudo” gold standard. The fiber orientation distribution function (ODF) was computed using a q-ball imaging algorithm. Root mean squared errors (RMSE) of ODF were compared.

Results

At 1 mm^3 voxel resolution, RSA produced reasonable DW images (Fig. 1b), whereas no diffusion signal was detectable in SS-SE-EPI (Fig. 1c). In RSA images, the blade sampling with composite reconstruction showed a subtle ringing artifact (Fig. 2) that was not observed in the full k-space EPI images. At the ideal SNR (Fig. 2 left column), the ringing artifact was less noticeable at a higher spatial resolution than at a regular voxel size of 2^3 mm^3 . The artifact was embedded in the noise and almost invisible at an SNR ≤ 30 , a typical range for current dMRI (Fig. 2)³. Consistent with a previous report, no obvious ringing artifacts were observed in the composite reconstructed brain images¹. The intensity of the artifact also remained small and similar across RSA AFs, suggesting it was not affected by the blade width. The RMSE between RSA and EPI images of Shepp-Logan phantom was $\sim 2\%$ and did not differ significantly across voxel sizes and SNRs. The PSF of the RSA approach had a slightly wider base (Fig. 3a, arrows) compared to EPI (Fig. 3b), which may explain the slight blurring in the composite reconstructed DW images of the brain¹. The effective resolution (i.e., FWHM of PSF) of RSA, however, seemed to have minimal impact (Table 1). Regardless of the AF and voxel sizes, the ratio of the nominal resolution to the effective resolution was approximately 1.2. Because geometric distortion and the T2* blurring effects of short-axis EPI blades are reported², we focused the computer simulation on artifacts arising from the blade sampling and composite reconstruction. Fig. 4 shows the ODF profiles reconstructed from RSA for three representative voxels with a single fiber orientation along x, y, and z axes at the corpus callosum, posterior corona radiata, and internal capsule, respectively. The overall RMSEs of ODF profiles between blade sampling with composite reconstruction and full k-space sampling were $< 3\%$ with a standard variation of $\sim 1.2\%$ across ~ 700 WM voxels (Fig. 5).

Discussion and Conclusions

Composite reconstruction is key to restoring spatial resolution along the frequency encoding direction (i.e., short-axis) of the k-space blades. Composite reconstruction of the RSA approach differs from that in the highly constrained backprojection⁴ approach with respect to image artifacts (ringing vs. streak) and the sparsity requirement (none vs. yes). The Nyquist criteria are fulfilled with RSA k-space blades; therefore, sparsity is not required. A 20% discrepancy between the effective and nominal resolution suggests a higher initial nominal resolution is preferred to minimize absolute resolution differences. This and the results of ringing artifacts are consistent and complement previous reports that RSA works better with higher spatial resolution. Based on post-processing simulation results with SS-SE-EPI as a “pseudo” gold standard, blade sampling with composite reconstruction in the RSA approach seemed to produce a reasonable estimate of fiber orientation with minimal RMSE.

References: 1. Wu et al. ISMRM 2014;666; 2. Skare et al. MRM 2006;55:1298-1307; 3. Wu et al. Neuroimage 2007;36(3):617-29; 4. Mistry et al. MRM 2006;55(1):30-40.

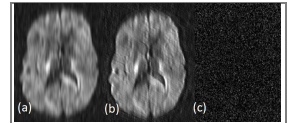


Fig. 1 DW images with voxel size of 1 mm^3 . (a) Low resolution image of k-space blade. (b) Composite reconstructed high resolution RSA image. (c) Conventional SS-SE-EPI.

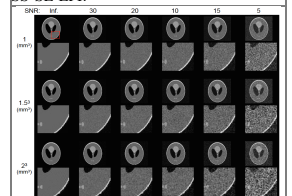


Fig. 2 Shepp-Logan brain phantom

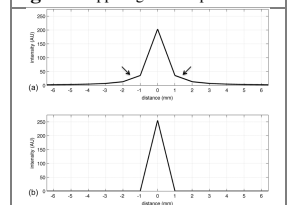


Fig. 3 PSF of 1 mm^3 voxel size

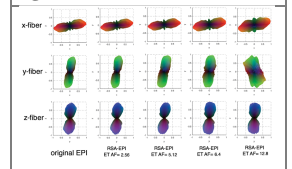
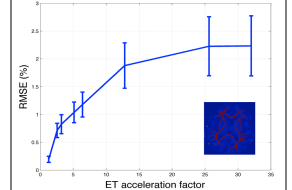


Fig. 4 ODF profiles. Color codes: L-R: red; A-P: green; and S-I: blue.



Nominal resolution (mm)	EPI	RSA				
		AF=2	AF=4	AF=8	AF=16	AF=32
1.00	1.01	1.19	1.21	1.22	1.22	1.22
1.50	1.50	1.73	1.75	1.77	1.77	1.77
2.00	2.02	2.38	2.41	2.43	2.44	2.44